Development 128, 4923-4933 (2001)
Printed in Great Britain © The Company of Biologists Limited 2001
DEV7913

The *Drosophila ribbon* gene encodes a nuclear BTB domain protein that promotes epithelial migration and morphogenesis

Katherine Shim[1], Kimberly J. Blake[2,*], Joseph Jack[2,‡] and Mark A. Krasnow[1,§]

[1]Howard Hughes Medical Institute and Department of Biochemistry, Stanford University, Stanford, CA 94305-5307, USA
[2]Department of Anatomy, University of Connecticut Health Center, Farmington, CT 06030, USA
*Present address: Mitchell College, New London, CT 06320, USA
‡Present address: 9 Cricket Lane, Simsbury, CT 06070, USA
§Author for correspondence (e-mail: krasnow@cmgm.stanford.edu)

Accepted 10 September 2001

SUMMARY

During development of the *Drosophila* tracheal (respiratory) system, the cell bodies and apical and basal surfaces of the tracheal epithelium normally move in concert as new branches bud and grow out to form tubes. We show that mutations in the *Drosophila ribbon* (*rib*) gene disrupt this coupling: the basal surface continues to extend towards its normal targets, but movement and morphogenesis of the tracheal cell bodies and apical surface is severely impaired, resulting in long basal membrane protrusions but little net movement or branch formation. *rib* mutant tracheal cells are still responsive to the Branchless fibroblast growth factor (FGF) that guides branch outgrowth, and they express apical membrane markers normally. This suggests that the defect lies either in transmission of the FGF signal from the basal surface to the rest of the cell or in the apical cell migration and tubulogenesis machinery. *rib* encodes a nuclear protein with a BTB/POZ domain and Pipsqueak DNA-binding motif. It is expressed in the developing tracheal system and other morphogenetically active epithelia, many of which are also affected in *rib* mutants. We propose that Rib is a key regulator of epithelial morphogenesis that promotes migration and morphogenesis of the tracheal cell bodies and apical surface and other morphogenetic movements.

Key words: *Drosophila*, *ribbon*, BTB/POZ domain, Pipsqueak domain, Trachea, Branching morphogenesis, FGF, Epithelial migration

INTRODUCTION

Many crucial events in animal development occur by movement and morphogenesis of epithelia. Perhaps the simplest, at least conceptually, is spreading of an epithelial sheet, as in chick epiboly (Downie, 1976) and dorsal closure of the *Drosophila* embryo (Kiehart et al., 2000). Other events involve three-dimensional changes in epithelial structure, like the epithelial invaginations that drive formation of the three germ layers at gastrulation (Costa et al., 1993) and underlie sprouting of new buds during branching morphogenesis (Bard, 1990). Some epithelia undergo an extreme structural transformation at epithelial-mesenchymal transitions: the epithelium separates into individual motile cells and epithelial character is lost.

Because cells in an epithelium are attached, morphogenetic events require coordination of the behavior of cells located at different positions in the epithelium. These events also require coordination of the behaviors of different parts of each constituent cell. For example, the apical and basal surfaces of epithelial cells usually move together during morphogenetic events, but occasionally they show strikingly different behaviors. During epithelial invaginations, the apical surface constricts, while the basal surface expands (Fristrom, 1988). The coordination of events at the apical and basal sides of an epithelium is of special interest because, unlike isolated cells like fibroblasts, the environment on each side of an epithelial cell is very different. The composition of the extracellular matrix is distinct, and the signaling molecules and receptors that trigger the morphogenetic events are typically localized on one side (Kim, 1997).

The *Drosophila* tracheal (respiratory) system is a branched network of epithelial tubes that provides a tractable genetic system for analyzing epithelial morphogenesis (Manning and Krasnow, 1993; Samakovlis et al., 1996). Tracheal tubes are a simple epithelial monolayer, with the apical surface lining the lumen and the basal surface forming the tube exterior. Development of the tracheal system begins by invagination of 20 ectodermal placodes, each of which forms an epithelial sac of ~80 cells. Over an 8 hour period in mid-embryogenesis, six primary branches bud from each sac, followed by about two dozen secondary branches. Subsequently, hundreds of fine terminal branches sprout during the several days of larval life. All of these budding events take place without loss of epithelial integrity and in the absence of cell division or death (Samakovlis et al., 1996): the extensively branched network forms exclusively by epithelial migration and morphogenesis.

Dozens of genes have been identified that are required for tracheal branching (Manning and Krasnow, 1993; Metzger and Krasnow, 1999; Affolter and Shilo, 2000). These have begun to separate the morphogenetic process into genetically distinct steps. Several genes are required for the initial specification of tracheal cell fate and invagination to form tracheal sacs. Another set of genes is required to assign distinct fates to each branch primordium before budding begins. Yet, other sets of genes are required for sprouting of primary, secondary and terminal branches.

Three primary branch genes have been characterized – *branchless* (*bnl*), *breathless* (*btl*) and *stumps* (*sms*). These encode components of a fibroblast growth factor (FGF) signaling pathway that directs budding and outgrowth of the primary branches. *bnl* encodes a FGF expressed by small clusters of cells surrounding each sac, at each position where a primary branch buds (Sutherland et al., 1996). Bnl serves as a chemoattractant, activating the Btl FGF receptor, a receptor tyrosine kinase expressed on the tracheal epithelium (Klambt et al., 1992). This directs budding and outgrowth of primary branches to Bnl signaling centers. *sms* encodes a putative adapter molecule expressed in tracheal cells and appears to function downstream of Btl (Michelson et al., 1998; Vincent et al., 1998; Imam et al., 1999). The FGF pathway also plays important roles controlling subsequent sprouting events. It induces expression of some secondary (e.g. *pointed*) and terminal branching genes (e.g. *blistered*/DSRF) in cells located at the ends of outgrowing primary branches, which go on to form secondary and ultimately terminal branches (Sutherland et al., 1996).

We have characterized a fourth primary branch gene, *ribbon* (*rib*). Although the gross phenotype of *rib* mutants is similar to that of *bnl*, *btl* and *sms*, cellular analysis shows that there is not a complete block to primary branch outgrowth. Basal cytoplasmic extensions still form and grow towards Bnl signaling centers, but there is a severe impediment in the migration and morphogenesis of the tracheal cell bodies and apical surface. *rib* has previously been implicated in several epithelial morphogenetic events (Nusslein-Volhard et al., 1984; Jack and Myette, 1997; Blake et al., 1998; Blake et al., 1999). We show that *rib* encodes a putative transcription factor expressed in the trachea and other morphogenetically active epithelia, and we propose that it functions as a regulator of epithelial migration and morphogenesis.

MATERIALS AND METHODS

Fly strains

rib^{1}, rib^{2} and rib^{z1} have been described elsewhere (Nusslein-Volhard et al., 1984; Blake et al., 1998). *Df(2R)*rib^{ex12} was generated by moblization of Terminal-3 P[w^{+},*lacZ*] transposon (Samakovlis et al., 1996) (K. Guillemin, PhD thesis, Stanford University, 1998). rib^{ex12} failed to complement the lethality of *l(2)k08810*, a lethal P insertion in *proliferation disrupter* (*prod*) (Torok et al., 1997); $enabled^{1-8}$ (enb^{1-8}) and enb^{87} (Gertler et al., 1995); *l(2)08713*, a lethal P insertion near *coracle* (*cora*); and rib^{1}, rib^{2}, rib^{z1}, rib^{P7} and rib^{P16}. Southern blot analysis indicated that the centromere-proximal breakpoint of rib^{ex12} lies between the Terminal-3 P[w^{+},*lacZ*] insertion site and *prod*, within 40 nucleotides 5′ to genomic sequence 5′-TGGCCAACTCTTCCTC. The distal breakpoint lies beyond *rib* but was not precisely defined.

Df(2R)P34 and *Df(2R)PC29* (Lindsley and Zimm, 1992) (http://flybase.bio.indiana.edu/), and *Df(2R)GC8* and enb^{GC1} (Gertler et al., 1995) are siblings generated from the same parental strains. The GAL4/UAS system (Brand and Perrimon, 1993) was used to misexpress *bnl*, using the 69B-GAL4 driver, which is expressed broadly in the embryo, and UAS-bnl^{B4-2} (Sutherland et al., 1996).

Mutagenesis

Isogenized *dp cn bw* males (aged 1-3 days after eclosion) were treated with 25 mM ethyl methane sulfonate (EMS) overnight and mated to *sco/CyO* females for 3-5 days (L. Messina, B. Lubarsky and M. A. K., unpublished). *dp cn bw* [*]*/CyO* progeny were tested: two out of 2086 mutagenized chromosomes screened failed to complement the lethality of rib^{ex12}, rib^{1} and rib^{2}, and were named rib^{P7} and rib^{P16}.

Antibodies and immunostaining

Embryo fixation and immunostaining were as described (Samakovlis et al., 1996). Primary antisera were TL1 and mAb 2A12 against tracheal lumenal antigens (Samakovlis et al., 1996), mAb 2-161 against DSRF (1:1000 dilution, from M. Gilman), anti-diphosphorylated-ERK (1:500, Sigma) and anti-β-galactosidase (1:1500, Cappel). Tracheal cells were visualized by staining embryos carrying the *1-eve-1* P[*lacZ*] insertion (Perrimon et al., 1991) with anti-β-galactosidase. Embryos were visualized with a Zeiss Axiophot microscope under Nomarski optics or a Molecular Dynamics MultiProbe 2010 laser scanning confocal microscope. For confocal fluorescence microscopy, *1-eve-1* embryos were stained with anti-β-galactosidase and anti-Crumbs mAb Cq4 (1:1000) (Tepass et al., 1990). Signal was developed by horseradish peroxidase (HRP)-catalyzed deposition of either cyanine 3- or fluorescein-labeled tyramide reagent (NEN Life Science Products).

Polyclonal rabbit anti-peptide antisera were raised against synthetic peptides in Rib (Research Genetics, Huntsville, AL). Antisera (Ab21802K) generated against the C-terminal peptide P3 (LKRELMEGEDAQARAD, Fig. 5) from two separate rabbits gave a similar staining pattern in whole-mount embryos. Antisera (Ab21083M) from a rabbit immunized with two peptides, P1 (TKSQEPEILRTAKELQVK) and P2 (EKHEQNIIKRERDQDERE-DA), gave a similar pattern. The α-Rib antisera were used at 1:1000 dilution and developed by HRP immunohistochemistry or HRP-catalyzed fluorescein tyramide reagent deposition and counterstained with DAPI (1 μg/ml in glycerol mounting medium) (Patel, 1994).

RNA in situ hybridization

In situ hybridization of whole-mount embryos was carried out with digoxigenin-labeled, single-stranded RNA probes and developed by alkaline phosphatase immunohistochemistry (Kopczynski et al., 1996). *bnl* probe was synthesized from Z3-2 cDNA (Sutherland et al., 1996); *btl* probe was synthesized from pDS7064 (from D. Sutherland), which contains a 3.3 kb *Eco*RI fragment containing the entire Btl-coding region. *rib* probe was a mixture of two overlapping probes synthesized from pKS3a and pKS4e, spanning a 1.6 kb region of *rib* between 5′-TGGTGGACGA and 5′-AGGGAGAACT. *rib* control probes against the antisense strand gave no signal.

Genetic mapping of *rib*

Meiotic recombination in a $cora^{2}$,+/+,rib^{1} transheterozygote was scored. Forty-two $cora^{+}rib^{+}$ chromosomes were generated out of 70,073 chromosomes screened. DNA sequencing in the genomic interval between *cora* and *rib* identified five polymorphisms (PM1-5) between the $cora^{2}$ and rib^{1} chromosomes (rib^{1} chromosome sequence shown in bold): PM1 (at 21 kb in Fig. 4C) GC(A/**G**)CGAATTTCTA (*Hha*I site underlined); PM2 (at 28 kb) TTA**ATGTTAAAGAC**TTAG (bold region deleted in $cora^{2}$ chromosome, *Dde*I site underlined); PM3 (at 40 kb) CT(T/**G**)CAGGTCAAGGG (*Pst*I); PM4 (at 70 kb) GAATCT(C/**T**)TT(T/**C**)TTGCACA (*Xmn*I); and PM5 (at 92 kb)

GAG(A/**C**)TCCACTCGAG (*Sac*I). *cora*$^{+}$*rib*$^{+}$ recombinant chromosomes were scored for the polymorphisms by restriction digestion with the indicated enzymes of PCR fragments containing the polymorphic sites.

To map the centromere-proximal endpoint of *Df(2R)GC8* and the distal endpoint of *Df(2R)P34*, PCR fragments ranging from 300-600 bp were amplified from genomic DNA prepared from heterozygous *Df(2R)GC8/CyO* and *Df(2R)P34/CyO* flies and their sibling control chromosomes *enb*^{GC1}*/CyO* and *Df(2R)PC29/CyO*, respectively. PCR products were purified and sequenced using dideoxy chain terminator chemistry on a capillary electrophoresis DNA sequencer (ABI310, Applied Biosystems). The presence of overlapping nucleotide peaks on the sequence chromatogram, confirmed by sequence of both strands, identified polymorphisms between the test chromosome (*Df(2R)GC8*, *Df(2R)P34*, *enb*^{GC1} or *Df(2R)PC29*) and the *CyO* balancer chromosome. The presence of a polymorphism in both a deficiency (e.g. *Df(2R)GC8/CyO*) and its sibling control (e.g. *enb*^{GC1}*/CyO*) PCR products indicated that this region was not deleted in the deficiency, whereas selective absence of a polymorphism in the deficiency PCR product was taken as evidence that the region was deleted. Polymorphisms present in both *Df(2R)GC8* and *enb*^{GC1} were: ATG(A/C)TCCCTT, AAT(G/T)GAAGCTGATT, CTC(C/G)GAATA-TGTGCTG, CAT(A/G)AGTTTCTTAC (PCR product 1; Fig. 4); CGC(A/C)C(A/C)AACCCATT, GCG(A/C)TATTGCAAC (product 2); ACACGCTGGAACA$_9$* (product 3); and TCC(C/G)ACCCGAA-AGC (product 4). Polymorphisms present in *enb*^{GC1} but absent in *Df(2R)GC8* were CGA(A/G)CTCAGGGTTTGC and ATA(G/T)AG-GCCCAAATTGC (product 5). Polymorphisms present in both *Df(2R)PC29/CyO* and *Df(2R)P34/CyO* were CTAAAAAAAA(C/-A)(T/A)* (product 8); GAGAGAGAAATA(T/G)* (product 9); (C/T)-ATGATGTGCG, (A/T)ATGAGTGCCC, (C/G)CCGGGAGCTG and (C/T)GCTGCGGCAG (product 10); and AATA(T/A)TTGAC (product 11). Polymorphisms present in *Df(2R)PC29/CyO* but absent in *Df(2R)P34/CyO* were TTCG(C/A)AAG (product 6) and (C/A)-AAGATGCCC and GAAAAAAAAA(G/A)(G/A)AA* (product 7). PCR products are numbered from left to right as shown in Fig. 4B. The asterisks above indicate that beyond this point in the sequence chromatogram there were multiple apparent polymorphisms presumably due to a deletion or insertion.

Molecular biology

A full-length *rib* cDNA (LD16058; Research Genetics) was sequenced (GenBank Accession Number, AF416603). NCBI tBLASTn homology searches (www.ncbi.nlm.nih.gov), Baylor College of Medicine BEAUTY post-processing (searchlauncher.bcm.tmc.edu) and InterPro pattern prediction searches (www.ebi.ac.uk) were used to identify BTB/POZ and Pipsqueak motifs.

To identify mutations in *rib* EMS alleles, DNA fragments (0.6-1 kb) spanning the *rib*-coding sequence and intron-exon junctions were amplified by PCR using genomic DNA isolated from *rib*^{1}/CyO, *rib*^{2}/CyO, *rib*^{z1}/CyO, *rib*^{P7}/CyO and *rib*^{P16}/CyO adult flies as template. PCR products were sequenced and polymorphisms between the *rib* and CyO chromosomes were identified as overlapping peaks on the sequence chromatogram. Because *rib*^{1}, *rib*^{2} and *rib*^{z1} were derived from isogenic parents, as were *rib*^{P7} and *rib*^{P16}, polymorphisms unique to a particular *rib* allele were assumed to be EMS-induced mutations. Putative EMS-induced mutations were confirmed by sequence of two independent PCR products.

RESULTS

Tracheal branches fail to form in *rib* mutants

Imprecise excision of the Terminal-3 P[w^{+},*lacZ*] tracheal marker at cytological position 56A-B generated a mutation (*ex12*) that severely impaired tracheal branch outgrowth. In wild-type embryos, all primary branches have grown out and the dorsal trunk branches have fused by stage 13, as seen by staining with tracheal antiserum TL1 (Fig. 1A,B). In *ex12* mutants, there was little branch outgrowth, and the trachea remained as a series of elongate, mostly unbranched sacs (Fig. 1C), similar to *bnl* null mutants at this stage (Fig. 1E). The block in branch outgrowth in *ex12* mutants was not absolute because after stage 14, although 99% of tracheal branches (*n*=180) remained stalled, 1% formed and grew out excessively and in aberrant directions (Fig. 1G,H). By stage 14, several other morphogenesis defects became apparent, including

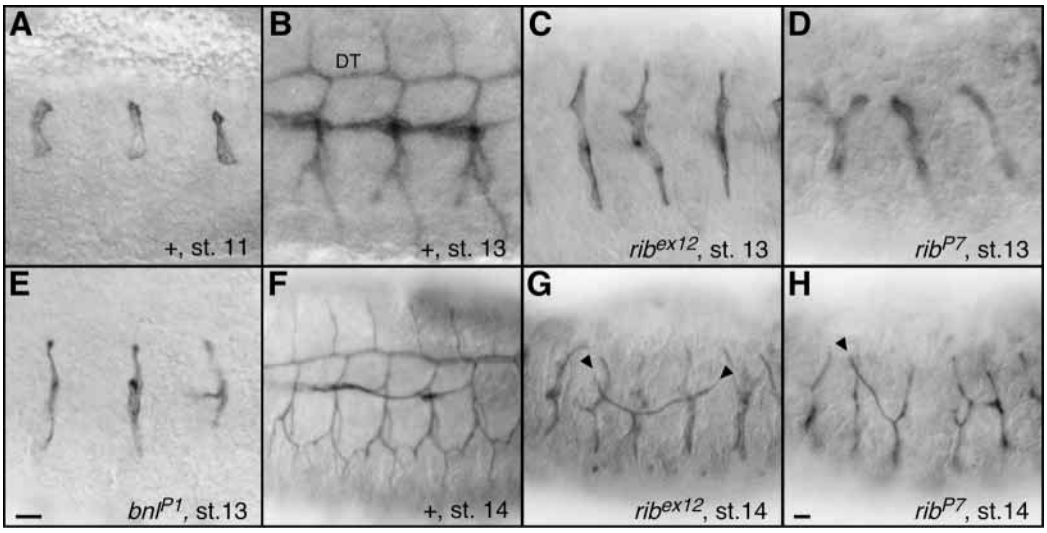

Fig. 1. Effect of *rib* mutations on tracheal branch outgrowth. (A) Three tracheal sacs in stage 11 wild-type (+) embryo stained with TL1 antiserum to show apical surface (lumen) of tracheal epithelium. (B) Similar view of stage 13 wild-type embryo. Primary branches have budded and dorsal trunk (DT) branches have fused. (C,D) Stage 13 *rib*^{ex12} and *rib*^{P7} homozygotes. Little branch budding or outgrowth has occurred. (E) Stage 13 *bnl*^{P1} homozygote for comparison. (F) Five tracheal metameres of stage 14 wild-type embryo. (G,H) *rib*^{ex12} and *rib*^{P7} homozygotes at similar stage. Outgrowth of most branches is stalled, but there is rare aberrant branch outgrowth (arrowheads). All panels in this and other figures show lateral views (dorsal upwards, anterior leftwards) unless noted. Scale bars: in E, 10 μm in A-E; in H, 10 μm in F-H.

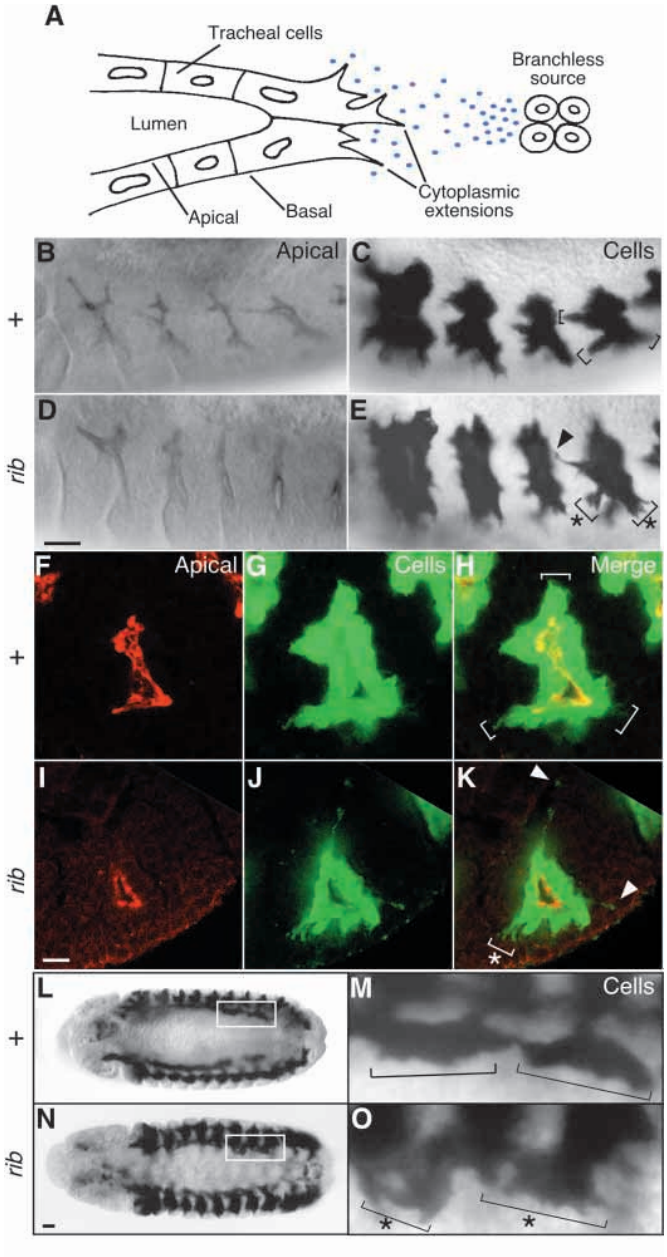

Fig. 2. Basal surface of tracheal epithelium continues to migrate in *rib* mutants. (A) Budding primary branch growing toward Bnl FGF signaling center. Cytoplasmic processes extend from the basal surface of the lead cells, and cell bodies and apical surface follow. (B,D) Four tracheal metameres (Tr1-4) of stage 12 rib^{+} (B) and rib^{ex12} (D) embryos stained with TL1 antiserum to show lumen and apical surface. Note limited outgrowth of apical surface in *rib* mutant. (C,E) Same view of similarly staged rib^{+} and rib^{ex12} embryos carrying *trachealess-lacZ* reporter (*1-eve-1/+*) and immunostained for β-galactosidase to show tracheal cells and basal surface. Basal cytoplasmic processes extend from the tips of growing branches (brackets) in both rib^{+} and rib^{ex12} embryos; the processes are sometimes more numerous (asterisks) and longer (arrowhead) in the mutant. (F-K) Confocal fluorescence micrographs of tracheal metamere Tr5 in stage 12 rib^{+} (F-H) and rib^{ex12} (I-K) embryos carrying *trachealess-lacZ* (*1-eve-1/+*) and double stained for the apical marker Crumbs and for β-galactosidase to show cells and basal surface. Red (Crumbs) channel (F,I), green (β-galactosidase) channel (G,J), and merged image (H,K). Cytoplasmic processes extend from the tips of growing branches (brackets) in both rib^{+} and rib^{ex12} embryos. Processes are sometimes more numerous (asterisk) and longer (arrowheads) in the mutant. (L-O) Ventral view (anterior left) of stage 13 rib^{+} (L,M) and rib^{ex12} (N,O) embryos carrying *trachealess-lacZ* (*1-eve-1/+*) and immunostained for β-galactosidase. Visceral tracheal branches (boxed in L,N) migrate internally onto the gut. Detail of boxed regions (M,O) show two visceral branches on the gut surface; cytoplasmic processes are more numerous in mutant. Scale bars: in D, 20 μm for B-E; in I, ~40 μm for F-K; in N, 20 μm for L,N.

failure of epidermal dorsal closure and midgut constriction formation (not shown).

Complementation tests with genes in cytological region 56A-C and molecular characterization of *ex12* (see Materials and Methods and below) indicated that the excision removed a number of genes including *rib*, so we call it $Df(2R)rib^{ex12}$ or rib^{ex12} for short. Loss of *rib* function was responsible for the tracheal phenotype, because rib^{1} and rib^{2} homozygotes, as well as rib^{1}/rib^{ex12} and rib^{2}/rib^{ex12} embryos all showed similar defects in branch outgrowth. This suggests that rib^{1} and rib^{2} are strong loss of function or amorphic (null) alleles. We identified two new mutations in *rib* (rib^{P7} and rib^{P16}) by screening 2086 second chromosomes carrying EMS-induced lethal mutations for failure to complement rib^{ex12} or rib^{1}. These too showed tracheal outgrowth defects (Fig. 1D,H), although the defects in rib^{P16} were much less severe (data not shown), implying that it is a weaker allele. Consistent with this, unlike the other *rib* alleles, which are all 100% homozygous lethal, a small number of $rib^{P16}/Df(2R)P34$ (2.2% of expected, *n*=180), rib^{P16}/rib^{1} and rib^{P16}/rib^{2} (2.7%, *n*=297) escapers survived to adulthood.

The basal surface of the tracheal epithelium continues to migrate in *rib* mutants

The TL1 tracheal antiserum used in the above experiments stains the apical surface and lumen of the developing tracheal epithelium. To further characterize the tracheal migration defects, we examined rib^{1}, rib^{2}, and rib^{ex12} mutants using the tracheal cytoplasmic marker *1-eve-1*, a viable P[*lacZ*] insert in *trachealess*. We found that despite the severe defect in movement of the apical tracheal surface described above, the basal surface continued to extend actively in the mutants.

A schematic diagram of a migrating tracheal branch is shown in Fig. 2A. In wild type, the basal surface of the tracheal epithelium is broad and smooth with an occasional pseudopodium extending from cells at the growing tip, much like those seen at the leading edge of migrating fibroblasts (Fig. 2C,G,H,M). As the basal surface extends toward the Bnl FGF signaling centers, the cell bodies and apical surface follow (Fig. 2B,F), and basal cytoplasmic extensions are never very prominent. In *rib* mutants, pseudopodia still extended from the basal surface (Fig. 2E,J,K,O), and were more numerous and pronounced than in wild type (asterisks in Fig. 2E,K,O), occasionally forming extremely long processes that appeared to reach their normal targets (arrowheads in Fig. 2E,K). This dissociation of the migration of the apical and basal tracheal surfaces was evident at stage 12 and continued for several hours into stage 14 (data not shown). At this later stage, the apical surface began to deform in the direction of the basal cytoplasmic extensions, but even at this later stage the net

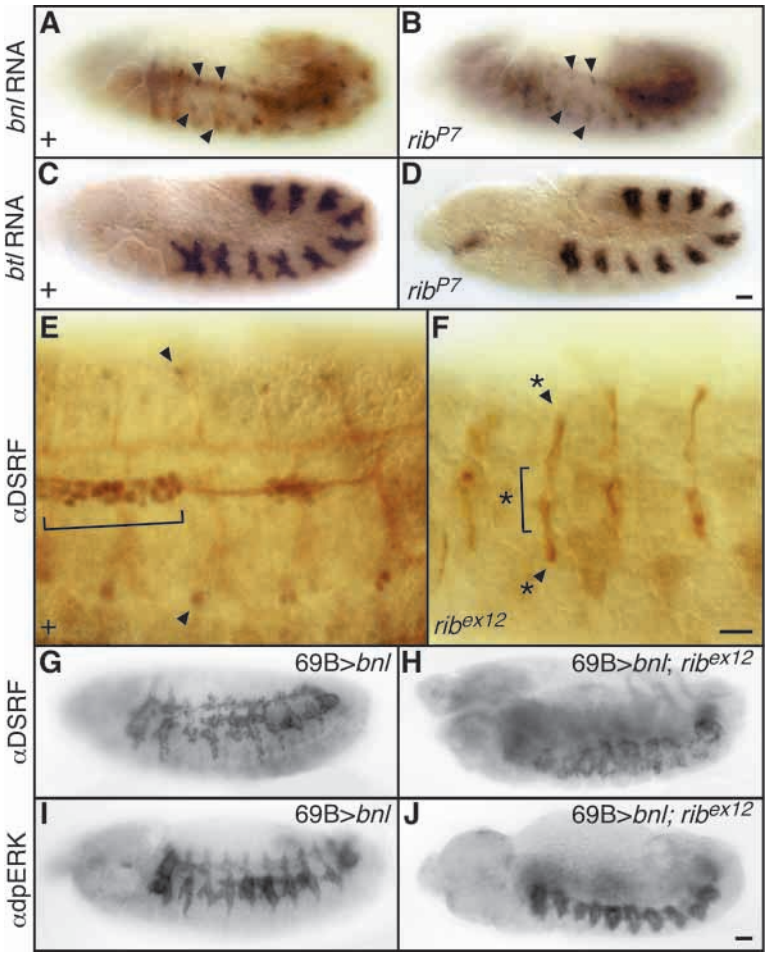

Fig. 3. Bnl FGF pathway gene expression and function in *rib* mutants. (A) In situ hybridization for *bnl* FGF mRNA (blue) in stage 12 heterozygous *rib*$^{+}$ embryo (*rib*^{P7}*/CyO,ftz-lacZ*). (Out-of-focus brown staining is immunostaining for β-galactosidase from *ftz-lacZ*.) (B) Same view of *rib*^{P7} homozygote. *bnl* mRNA expression pattern is not grossly affected. Arrowheads, *bnl* expression domains 3′, 3, 4, 5/7 (Sutherland et al., 1996). (C) In situ hybridization for *btl* FGFR mRNA in stage 12 heterozygous *rib*$^{+}$ embryo (*rib*^{P7}*/CyO,ftz-lacZ*). (D) Same view of *rib*^{P7} homozygote. Tracheal branch outgrowth is stalled but *btl* mRNA is expressed normally. (E) Four tracheal metameres of wild-type embryo double stained for the 2A12 tracheal lumenal antigen (brown) and DSRF/*blistered*, a Bnl-induced gene (blue). DSRF expression is induced in cells at the ends of primary branches (bracket, arrowheads). (F) Same view of *rib*^{ex12} embryo. Tracheal branches do not grow out normally and DSRF expression is not induced (asterisks). (G) *UAS-bnl/+;69B-GAL4/+* embryo stained for DSRF. Ectopic *bnl* expression induces DSRF expression throughout the tracheal system. (H) *UAS-bnl/+; rib*^{ex12}*; 69B-GAL4/+* embryo stained for DSRF. Although the *rib* mutation blocks branch outgrowth, it does not prevent *bnl* induction of DSRF expression throughout the trachea. (To aid in embryo genotyping, this preparation was also stained for β-galactosidase expressed from a TM3 *Ubx-lacZ* balancer chromosome in the cross, and hence has higher background staining than G.) (I) *UAS-bnl/+; 69B-GAL4/+* embryo stained for diphospho-ERK. Ectopic Bnl expression activates ERK throughout the tracheal system. (J) Same view of *UAS-bnl/+; rib*^{ex12}*; 69B-GAL4/+* embryo. Although the *rib* mutation blocks branch outgrowth, it does not prevent *bnl*-induced phosphorylation of ERK throughout the trachea. Scale bars: in D, 20 μm for A-D; in F, 10 μm for E,F; in J, 20 μm for G-J.

distance traveled by the apical side was far less than in wild type. The apical defect is unlikely to reflect a general defect in apical-basal polarity of the tracheal epithelium because the apical determinant Crumbs (Tepass et al., 1990), the apical marker TL1, and an apically localized mRNA (K. S. and M. A. K., unpublished) were expressed and localized properly at the apical tracheal surface in *rib* mutants (Fig. 2D,I and data not shown). We conclude that *rib* mutations selectively affect movement and morphogenesis of the tracheal cell bodies and apical surface.

rib mutants can respond to Bnl FGF

We examined whether Bnl FGF signaling was affected in *rib* mutants. In situ hybridization for *bnl* and *btl* transcripts showed that both were expressed grossly normally in *rib*^{P7} embryos (Fig. 3B,D), a null allele of *rib* (see below). Furthermore, unlike *bnl*^{P1} mutants, in which only an occasional tracheal cytoplasmic extension was detected (data not shown), in *rib* mutants cytoplasmic extensions formed and grew towards their normal targets (Fig. 2E,K,N), implying that the Bnl pathway was active.

To examine more directly whether *rib*$^{-}$ tracheal cells can sense and respond to Bnl, we assayed downstream components in the Bnl signaling pathway. We found that expression of the terminal branch gene *blistered*/DSRF, which is normally induced by Bnl signaling at the ends of growing primary branches, was not induced to high levels in *rib* mutants (Fig. 3E,F). However, this appears to be a secondary consequence of the migration defect, because when a *bnl* transgene (UAS*bnl*) was expressed ubiquitously in *rib* mutants to expose the stalled tracheal cells to high concentrations of Bnl, MAPK was activated and *blistered*/DSRF expression was induced throughout the tracheal epithelium (Fig. 3H,J), as in *rib*$^{+}$ animals (Fig. 3G,I). We conclude that *rib* mutant tracheal cells can respond to Bnl. This suggests that the migration defect results from either an inability to transmit the Bnl signal from the basal surface to the cell bodies and apical surface, or an inability of the cell bodies and apical surface to respond once they receive the signal.

rib encodes a BTB domain protein

rib maps meiotically to 2-88 (Nusslein-Volhard et al., 1984). Complementation tests with deficiencies in the region placed *rib* in cytological interval 56B5 to 56C1 (Fig. 4A). The left and right endpoints of this interval were defined molecularly (Fig. 4B). This was done by scanning the region for single nucleotide polymorphisms (SNPs) that distinguished sibling deficiency chromosomes from the *CyO* balancer chromosome. Polymorphisms that were missing in *Df(2R)GC8* or *Df(2R)P34* chromosomes over the balancer were assumed to be due to deletion of that region in the deficiency chromosome. This localized *rib* to an ~150 kb interval between 5-HT1A receptor gene and predicted gene CG7230 (Fig. 4B).

The position of the *rib*^{1} mutation was refined by meiotic

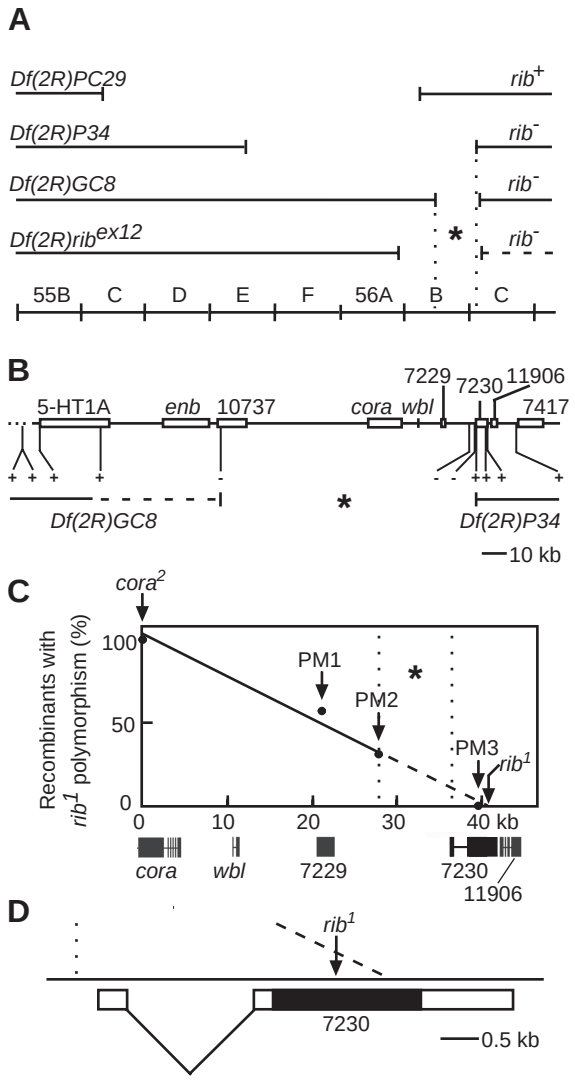

Fig. 4. Genetic mapping of *rib*. (A) Map of deficiencies in the 55B-56D region and their lethal complementation behavior with *rib* (at least three *rib* alleles were tested). *rib* maps to the interval (*) between the left endpoint of *Df(2R)GC8* (56B5) and the right endpoint of *Df(2R)P34* (56C1). (B) Sequence polymorphism mapping of the left endpoint of *Df(2R)GC8* and right endpoint of *Df(2R)P34*. Region deleted (–) or present (+) in *Df(2R)GC8* or *Df(2R)P34* chromosome as indicated by the absence (–) or presence (+) of a sequence polymorphism at that position (see Materials and Methods). Positions of some known and predicted genes (indicated by CG number) are shown. (C) Meiotic recombination mapping of rib^1 with respect to $cora^2$. $cora^+ rib^+$ recombinant chromosomes (n=42) resulting from a crossover between $cora^2$ and rib^1 in a $cora^2,+/+,rib^1$ transheterozygote were genotyped for five polymorphic markers (PM1-5) in the region. The percentages of recombinant chromosomes carrying the rib^1 chromosome allele of PM1, PM2 and PM3 are shown. None carried the rib^1 chromosome allele of PM4 or PM5, which map further to the right (not shown). This mapped rib^1 to the right of PM2 (dotted line at 28 kb), in an ~9 kb interval (*) bounded by the right endpoint of *Df(2R)P34* (dotted line at 37 kb). Extrapolation (broken line) places rib^1 in the CG7230 locus. Positions of transcripts in the region are shown.
(D) Organization of CG7230 locus and cDNA. Boxes, exons; black, coding region; dotted line, right endpoint of *Df(2R)P34*; broken line, extrapolated position of rib^1 (from C); arrow, actual position of rib^1 mutation (see Fig. 5A).

recombination mapping with respect to $cora^2$ and five nearby polymorphic markers including PM1 and PM2 (Fig. 4C). rib^1 mapped 0.12 cM to the right of $cora^2$, 0.07 cM to the right of PM1 and 0.03 cM to the right of PM2. This localized rib^1 to a ~9 kb region (+28 to +37 kb in Fig. 4C) at the extreme right end of the 150 kb interval defined by deficiency mapping. CG7230 is the only transcription unit in the 9 kb region, and extrapolation of the recombination mapping data predicted that rib^1 lies within the CG7230 transcription unit (Fig. 4C,D).

To confirm that CG7230 is *rib*, we sequenced the CG7230-coding region and intron-exon junctions of the five *rib* EMS alleles. CG7230 encodes a protein with a BTB (Bric à brac, Tramtrack, Broad) domain and a Pipsqueak (Psq) DNA-binding motif (see below). All five *rib* alleles contain mutations that remove or alter a conserved element in the protein (Fig. 5A). rib^1 and rib^{P7} carry nonsense mutations that truncate the predicted protein at residues 22 and 283, respectively, removing half or more of the protein and one or both functional motifs, consistent with their assignment as amorphic alleles. rib^2 and rib^{z1} carry an identical missense mutation which changes a highly conserved arginine (Arg58) in the BTB domain (Ahmad et al., 1998) to histidine. This change is apparently highly deleterious because both alleles behave as amorphic alleles. rib^{P16}, a hypomorphic allele, carries a missense mutation that changes Ser389 in the predicted Psq DNA-binding motif to cysteine. We also showed by whole-mount in situ hybridization that CG7230 transcript is absent in *Df(2R)P34* embryos (data not shown), so although the deficiency does not impinge on CG7230 coding sequence (Fig. 4D), it must remove essential regulatory elements. The coding regions of the two genes flanking CG7230 (CG7229 and CG11906) were also sequenced in the rib^{P7} and rib^{P16} alleles and no mutations were found. We conclude that CG7230 is *rib*.

An EST representing CG7230 was sequenced and compared with the *Drosophila* genomic sequence (Adams et al., 2000). Fig. 4D shows the deduced gene structure. There is a single predicted open reading frame that encodes a 661 residue (71 kDa) protein (Fig. 5A). There are stop codons in all three reading frames upstream of the coding sequence, implying that this is a complete coding sequence.

Blast sequence homology searches with the deduced Rib protein sequence identified a region similar to BTB (or POZ for Poxvirus and zinc finger) domains, a protein-protein interaction domain found in zinc finger transcription factors and actin-associated proteins of the *Drosophila* Kelch family (Bardwell and Treisman, 1994; Zollman et al., 1994). Like other BTB domains, the BTB domain in Ribbon is ~120 residues and located close to the N terminus. It shares 35-38% identity (~60% similarity) with three founding members of the BTB family, the *Drosophila* developmental regulatory proteins Bric à brac, Tramtrack and Broad-complex transcription factor (Fig. 5B). The BTB domain of Rib is slightly more similar (40% identity, 63% similarity) to the BTB domain of *longitudinals lacking* (*lola*), a zinc-finger nuclear factor implicated in axon growth and targeting in the *Drosophila* nervous system (Giniger et al., 1994). Other BTB domains show less identity, such as Kelch (25% identity) and human promyelocytic leukemia zinc finger (PLZF) protein (24% identity).

Many BTB domain proteins also contain a zinc-finger DNA-binding domain, but we were unable to identify a zinc finger

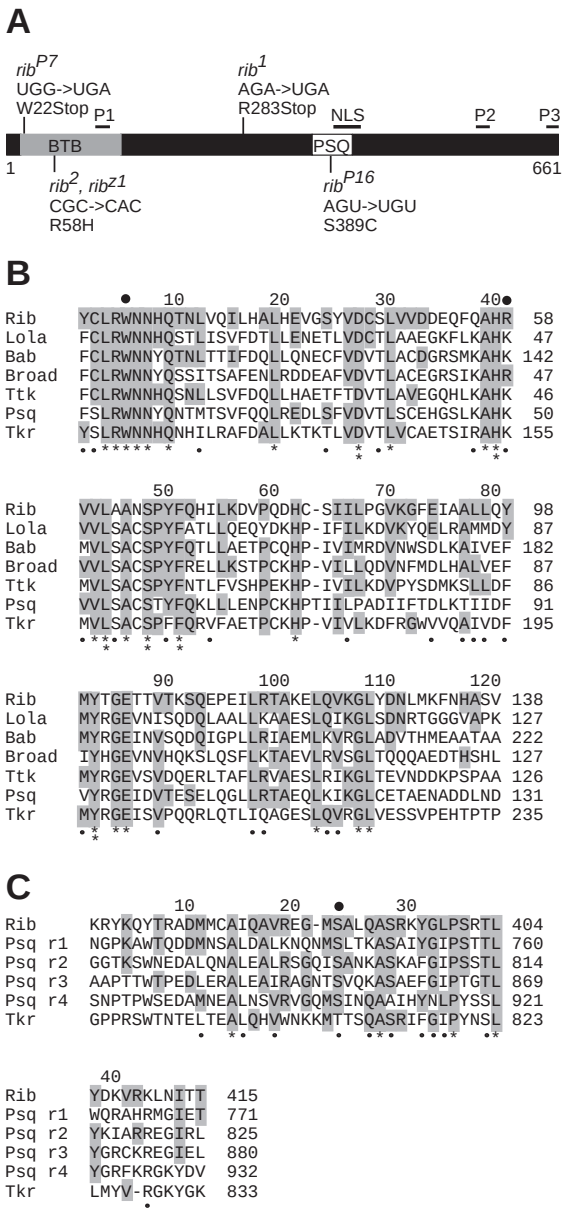

Fig. 5. Primary structure of Rib protein. (A) Diagram showing locations of BTB domain (residues 18-138, gray fill), Pipsqueak (PSQ) motif (367-415, white fill) and bipartite nuclear localization sequence (NLS, 395-412, 409-426). The positions and consequences of *rib*^{P7}, *rib*^{1}, *rib*^{2}, *rib*^{z1} and *rib*^{P16} mutations are indicated, as are locations of three peptides (P1,P2,P3) used to generate Rib antisera. (B) Sequence alignment of BTB domains of Rib, Longitudinals lacking (Lola), Bric à brac (Bab), Broad-complex (Broad), Tramtrack (Ttk), Pipsqueak (Psq) and Tyrosine kinase related (Tkr). Residues identical to Rib are shaded. Marks below sequence indicate residues identical (*) or similar (.) among proteins shown, or identical among all BTB domain proteins (*). Large black circle, locations of changes caused by *rib*^{P7} mutation and *rib*^{2} and *rib*^{z1} mutations. (C) Sequence alignment of Psq motifs in Rib, Psq and Tkr. Large black circle, location of *rib*^{P16} mutation.

motif in Rib using PROSITE. However, Blast/BEAUTY searches with the Rib-coding region revealed a 49 residue region (residues 367 to 415) with similarity to the DNA-binding domain of Psq, a protein involved in patterning the early *Drosophila* egg, embryo and adult eye (Weber et al., 1995; Horowitz and Berg, 1996). The Psq DNA binding domain consists of four tandem repeats of an ~50 amino acid motif (Lehmann et al., 1998), each of which is 30-48% identical to each other and 28-36% identical to the region in Rib (Fig. 5C). The Psq repeats also show similarity to the helix-turn-helix DNA-binding domain of a number of prokaryotic recombinases including *E. coli* Hin Invertase (Lehmann et al., 1998). A single Psq motif is found in *Drosophila* Tyrosine Kinase Related (Tkr) protein (Haller et al., 1987). Interestingly, both Psq and Tkr also contain N-terminal BTB domains (36% identity between the Psq and Rib BTB domains; 32% between Tkr and Rib). Psq, Rib, and Tkr thus define a new subtype of BTB domain proteins with a Psq DNA-binding motif.

rib is expressed in epithelia undergoing morphogenetic movements

rib expression during development was analyzed by in situ hybridization of whole-mount embryos (Fig. 6). *rib* transcript was detected in the developing tracheal system, as the tracheal precursor cells invaginate to form tracheal sacs and primary branches bud and grow out from the sacs (Fig. 6G and data not shown). *rib* was also expressed in a variety of other tissues, in a complex and dynamic pattern that coincides with various morphogenetic movements (Fig. 6C-J). For example, *rib* was first detected at stages 5-8 (~2.5-3.5 hours AEL) in the primordia of the anterior and posterior midgut as they invaginate to form tubes (Fig. 6B-D); expression turned on again in the tubes a couple hours later (stages 10-14, ~5-11 hours AEL) as they extend and form the central portion of the gut (Fig. 6H-J). *rib* expression was also seen in the developing mesoderm at or just after its ectodermal invagination and epithelial-to-mesenchymal transition, as the mesodermal cells begin their dorsal migration (~4 hours AEL; Fig. 6C,E). *rib* was also expressed in the stomodeum and proctodeum, as they invaginate to form the foregut and hindgut, and as the Malpighian tubules bud (Fig. 6E, H). *rib* was expressed broadly in the epidermis from stage 10 to 15 (~5-13 hours AEL) as it migrates during dorsal closure (Fig. 6I). Some of these sites of *rib* expression are also associated with morphological defects in *rib* mutants (see Discussion).

Although *rib* is expressed during many morphogenetic movements, some morphogenetic events are not associated with *rib* expression. For example, *rib* was not expressed strongly during cephalic furrow formation or formation of the anterior and posterior transverse folds (Fig. 6C,D).

Ribbon is a nuclear protein

Two polyclonal antisera were raised against non-overlapping peptides in Rib (Fig. 5A). In stains of whole-mount embryos, both antisera showed the same pattern of Rib protein expression, which followed the pattern of *rib* transcripts (Fig. 7A-D and data not shown). Staining is specific for Rib because it was absent in *rib*^{ex12} (Fig. 7F) and in *rib*^{P7}, a nonsense mutation that truncates the protein N-terminal to the epitopes. Rib staining showed a cellular distribution consistent with nuclear localization (Fig. 7A,C,E). This was confirmed by co-staining with the nuclear dye DAPI, which showed coincidence of Rib and DAPI staining except in regions near the centromere which stain intensely with DAPI (Hiraoka et al., 1990) but excluded Rib (Fig. 7G-I).

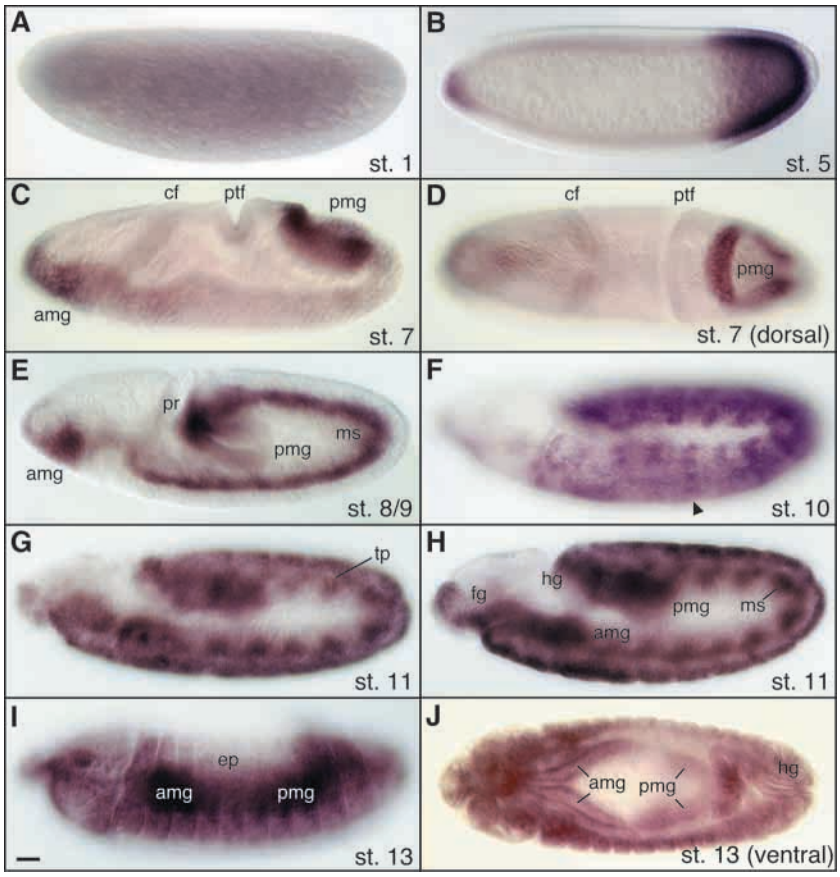

Fig. 6. Expression of *rib* mRNA. In situ hybridization of wild-type embryos with *rib* RNA probe at embryo stages indicated. (A) Stage 1 (0-15 minutes after egg lay). No transcript is detected. (B) Stage 5 (~3 hours). (C) Stage 7 (~3.5 hours). Note expression in cells invaginating to form anterior and posterior midgut (amg, pmg). (D) Dorsal view of same embryo. *rib* transcript is not detected in cells invaginating to form cephalic furrow (cf) and posterior transverse fold (ptf). (E) Stage 8/9 (~4 hours). Expression has turned off in the pmg and initiated in the proctodeum (pr) as it invaginates and in mesoderm as cells take on mesenchymal character and begin migration. (F) Stage 10 (~5 hours). *rib* expression has initiated throughout the epidermis and is enriched in segmental patches (arrowhead). (G) Stage 11 (~7 hours), surface view. Note *rib* expression in tracheal cells as they invaginate to form tracheal pits (tp). (H) Same as G, internal focal plane. Note *rib* transcript in the amg, pmg, foregut (fg) and hindgut (hg) regions, and mesodermal clusters (ms). (I) Stage 13 (~10 hours). *rib* is expressed throughout the epidermis (ep) as it spreads during dorsal closure. Transcript is also seen in the amg and pmg deep to the focal plane. (J) Stage 13, ventral view. *rib* transcript is present broadly throughout the embryo including the amg and pmg, as the cells migrate towards each other and form the central gut tube, and the hindgut as it elongates. Broad expression continues in stage 14 and 15 (not shown). Scale bar: 30 μm.

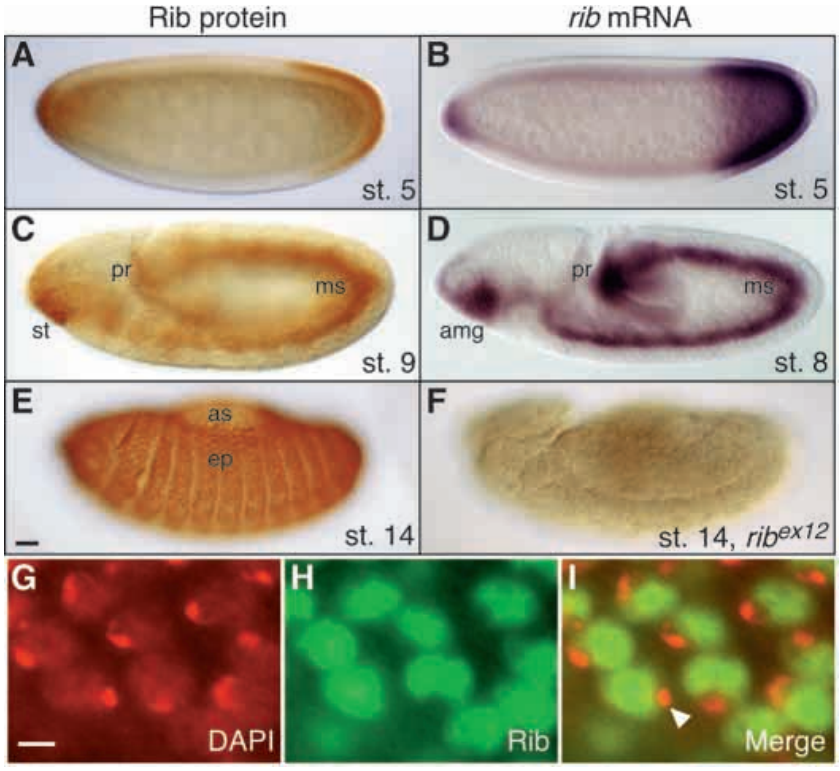

Fig. 7. Rib protein expression and localization. Wild-type (A,C,E) and rib^{ex12} (F) embryos stained with anti-Rib (P3) antiserum Ab21802K. No Rib expression is detected in mutant (F). (B,D) *rib* RNA distribution at similar stages for comparison. st, stomodeum; ms, mesoderm; pr, proctodeum; ep, epidermis; as, amnioserosa. (G-I) Detail of ventral epidermis in stage 14 embryo double stained with Rib antiserum (fluorescein) and DAPI. (G) DAPI channel. (H) Rib (fluorescein) channel. (I) Merged image. Rib staining is coincident with DAPI except for the centromeric region (arrowhead) which stains intensely only with DAPI. Scale bar: 30 μm in A-F; ~2 μm in G-I.

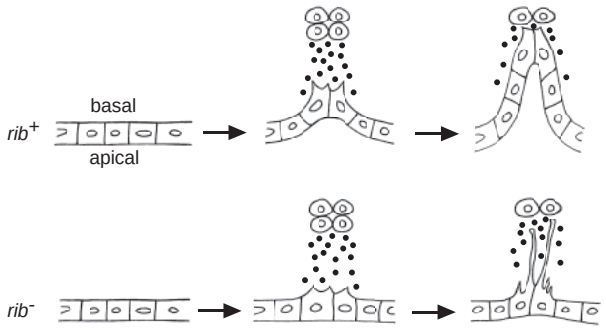

Fig. 8. Schematic of *rib* tracheal phenotype. In *rib* mutants, basal cytoplasmic processes extend toward Bnl signaling centers, but cell bodies and apical tracheal surface fail to follow.

DISCUSSION

rib is required for tracheal migration and tubulogenesis but not cytoplasmic extension

rib mutations impede budding and outgrowth of all primary tracheal branches, causing a severe phenotype grossly similar to that of mutations in *bnl*, *btl* and *sms*. These other genes encode components of a FGF signaling pathway that guides migration of the primary branches as they bud and assemble into tubes. The migrations are led by basal cytoplasmic extensions from tracheal cells located at the tip of each bud, which extend toward the Bnl/FGF signaling centers (Fig. 8, top). Whereas *bnl* mutations block both cytoplasmic extension and cell migration, we found that in *rib* null mutants the *bnl* pathway is active and cytoplasmic processes extend unimpeded. However, movement of the tracheal cell bodies and formation of new branches is profoundly affected (Fig. 8, bottom). Thus, *rib* identifies a new step in primary branch budding and outgrowth that lies downstream or parallel to *bnl* signaling.

What is this step? During primary branch budding, the basal surface of the tracheal epithelium is exposed to secreted Bnl/FGF, and the cells respond by extending pioneer cytoplasmic processes towards the Bnl source (Fig. 8, top). But for a new branch to form, the cell bodies and apical surface must follow. Unlike isolated cells like *Dictyostelium* or fibroblasts migrating up a chemoattractant gradient, where the entire cell is exposed to the attractant, the cell bodies and apical surface of the tracheal epithelium are sealed off and do not have direct access to Bnl. These parts of the cell must receive the stimulus to move indirectly. *rib* might be required for transmission of the Bnl signal from the basal surface to the rest of the cell or to otherwise couple their movement. Alternatively, *rib* may be needed to propel the cell body forward once it receives the signal to move. Fibroblasts use distinct molecular mechanisms to move their leading and trailing sides forward (Lauffenburger and Horwitz, 1996); perhaps *rib* is required for a myosin-dependent process like the one used to propel the trailing side of a migrating fibroblast forward. Rib might also be needed to promote the cell shape and apical surface changes necessary to form or extend a new tube. Although the data do not pinpoint the precise cellular event mediated by Rib, it is clear that the gene identifies a distinct step in tracheal branching – one that may be common to a number of other epithelial morphogenetic events.

Rib is a putative transcription factor

rib encodes a 71 kD protein with a BTB motif most similar to those found in other developmental regulatory proteins, and a separate motif similar to the DNA binding domain of Psq. The presence of two motifs found in transcription factors, together with the immunolocalization data showing that Rib is nuclear, suggest that Rib is a DNA-binding transcription factor that promotes tracheal migration and tubulogenesis by regulating the expression of target genes. Because BTB domains are known to serve as protein-protein interaction domains (Bardwell and Treisman, 1994), Rib may act as a homo- or heterodimer or higher order complex. Although its targets in the trachea are unknown, *rib* mutants affect the expression of the *zipper* myosin heavy chain in migrating epidermis during dorsal closure (Blake et al., 1998). Thus, *zipper* could be a target of Rib, at least in epidermis.

The genetic analysis indicates that *rib* functions downstream or parallel to the Bnl FGF pathway. If Rib functions downstream in the FGF pathway, for example, if its transcriptional regulatory activity is regulated by RAS/MAPK signaling like the Yan (Rebay and Rubin, 1995; Hacohen et al., 1998), DSRF (Guillemin et al., 1996) and possibly Pointed (Brunner et al., 1994) transcription complexes, then this would provide a natural way of coupling morphogenetic events in the tracheal cell bodies and apical surface to events at the basal surface, where the Bnl signal is received. When the Bnl pathway is active, the receptor would directly stimulate outgrowth of the basal tracheal surface. But it would also indirectly stimulate migration and morphogenesis of the cell body and apical surface – via activation of Rib and induction of its target genes.

Rib, together with the *Drosophila* proteins Psq and Tkr, defines a new subfamily of BTB proteins containing Psq DNA-binding motifs. Although most other BTB domain proteins are also believed to function as transcription factors, this much larger subfamily of BTB domain proteins all contain zinc-finger (ZF) DNA-binding motifs (Zollman et al., 1994; Albagli et al., 1995; Read et al., 2000). The BTB domains of BTB/Psq proteins are no more similar to each other than they are to those of BTB/ZF proteins, although they are more similar to each other than they are to the BTB domain of Kelch, a cytoplasmic protein. The reason for the common coupling of BTB domains with two structurally unrelated DNA binding motifs, but not other DNA binding motifs, is unclear.

rib functions in a variety of epithelial migration and morphogenesis events

In addition to the tracheal system, *rib* is expressed in a number of other developing tissues, in a complex and dynamic pattern that coincides with various morphogenetic movements. Several sites of expression coincide with epithelial invaginations or evaginations to form tubes or sacs, as occurs during tracheal branch budding. These sites include the anterior and posterior midgut invaginations, salivary gland primordia as they invaginate and extend, stomodeum and proctodeum as they invaginate to form the foregut and hindgut, and Malpighian (renal) tubules as they bud. *rib* is also expressed during spreading of a planar epithelium, the epidermis, during dorsal

closure. *rib* is expressed during or just after a number of mesenchymal-epithelial transitions, including the midgut mesenchyme as it reorganizes into an epithelium and forms the central portion of the gut.

Several of these morphogenetic events are defective in *rib* mutants. Indeed, *rib* mutants were first identified by their dorsal closure defect (Nusslein-Volhard et al., 1984). *rib* mutants also have defects in a number of other tissues including the Malpighian tubules, salivary glands and hindgut (Jack and Myette, 1997; Blake et al., 1998; Blake et al., 1999). Each of these are epithelia, and there are defects in the cell shape changes that underlie their morphogenesis. For example, *rib* mutant epidermal cells fail to elongate properly, and salivary gland cells fail to constrict apically (Blake et al., 1998).

Almost all epithelia undergoing morphogenetic movements face similar challenges as the tracheal epithelium during primary branching – different parts of the epithelium must move coordinately although they are exposed to different environments. Based on our analysis of the tracheal function of *rib*, as well as its expression and activity in a variety of other morphogenetic processes, we propose that Rib is a key regulator of the movement and morphogenesis of epithelia, particularly events in the cell bodies or apical surface during budding of tubular epithelia. In some migrating epithelia, such as the spreading epidermis during dorsal closure, it is not clear that *rib* mutations specifically disrupt an apical process, so Rib may also influence epithelial migration and morphogenesis in other ways. Insight into the mechanisms and molecules that execute these morphogenetic events may come through the identification of transcriptional targets of Rib.

Another characterization of *rib* appeared after review of this manuscript (Bradley and Andrew, 2001).

We thank L. Messina and B. Lubarsky for performing EMS mutagenesis; K. Guillemin for rib^{ex12}; R. Reenan for genomic sequencing; the Bloomington Stock Center, M. Gilman and B. Shilo for stocks and reagents; and members of the Krasnow laboratory for helpful discussion. This work was supported by an NSF Predoctoral Fellowship and NIH training grant (K. S.) and NSF grant IBN 9723791 (to J. J.). M. A. K. is an investigator of the Howard Hughes Medical Institute.

REFERENCES

Adams, M. D., Celniker, S. E., Holt, R. A., Evans, C. A., Gocayne, J. D., Amanatides, P. G., Scherer, S. E., Li, P. W., Hoskins, R. A., Galle, R. F. et al. (2000). The genome sequence of *Drosophila melanogaster*. *Science* **287**, 2185-2195.

Affolter, M. and Shilo, B. Z. (2000). Genetic control of branching morphogenesis during *Drosophila* tracheal development. *Curr. Opin. Cell Biol.* **12**, 731-735.

Ahmad, K. F., Engel, C. K. and Prive, G. G. (1998). Crystal structure of the BTB domain from PLZF. *Proc. Natl. Acad. Sci. USA* **95**, 12123-12128.

Albagli, O., Dhordain, P., Deweindt, C., Lecocq, G. and Leprince, D. (1995). The BTB/POZ domain: a new protein-protein interaction motif common to DNA- and actin-binding proteins. *Cell Growth Differ.* **6**, 1193-1198.

Bard, J. (1990). Morphogenesis: the cellular and molecular processes of developmental anatomy. Cambridge: Cambridge University Press.

Bardwell, V. J. and Treisman, R. (1994). The POZ domain: a conserved protein-protein interaction motif. *Genes Dev.* **8**, 1664-1677.

Blake, K. J., Myette, G. and Jack, J. (1998). The products of *ribbon* and *raw* are necessary for proper cell shape and cellular localization of nonmuscle myosin in *Drosophila*. *Dev. Biol.* **203**, 177-188.

Blake, K. J., Myette, G. and Jack, J. (1999). *ribbon*, *raw*, and *zipper* have distinct functions in reshaping the *Drosophila* cytoskeleton. *Dev. Genes Evol.* **209**, 555-559.

Bradley, P. L. and Andrew, D. J. (2001). *ribbon* encodes a novel BTB/POZ protein required for directed cell migration in *Drosophila melanogaster*. *Development* **128**, 3001-3015.

Brand, A. H. and Perrimon, N. (1993). Targeted gene expression as a means of altering cell fates and generating dominant phenotypes. *Development* **118**, 401-415.

Brunner, D., Ducker, K., Oellers, N., Hafen, E., Scholz, H. and Klambt, C. (1994). The ETS domain protein Pointed-P2 is a target of MAP kinase in the Sevenless signal transduction pathway. *Nature* **370**, 386-389.

Costa, M., Sweeton, D. and Wieschaus, E. (1993). Gastrulation in *Drosophila*: cellular mechanisms of morphogenetic movements. In *The Development of* Drosophila melanogaster. Vol. I (ed. M. Bate and A. Martinez Arias), pp. 425-465. Plainview: Cold Spring Harbor Laboratory Press.

Downie, J. R. (1976). The mechanism of chick blastoderm expansion. *J. Embryol. Exp. Morphol.* **35**, 559-575.

Fristrom, D. (1988). The cellular basis of epithelial morphogenesis. A review. *Tissue Cell* **20**, 645-690.

Gertler, F. B., Comer, A. R., Juang, J. L., Ahern, S. M., Clark, M. J., Liebl, E. C. and Hoffmann, F. M. (1995). *enabled*, a dosage-sensitive suppressor of mutations in the *Drosophila* Abl tyrosine kinase, encodes an Abl substrate with SH3 domain-binding properties. *Genes Dev.* **9**, 521-533.

Giniger, E., Tietje, K., Jan, L. Y. and Jan, Y. N. (1994). *lola* encodes a putative transcription factor required for axon growth and guidance in *Drosophila*. *Development* **120**, 1385-1398.

Guillemin, K., Groppe, J., Ducker, K., Treisman, R., Hafen, E., Affolter, M. and Krasnow, M. A. (1996). The *pruned* gene encodes the *Drosophila* serum response factor and regulates cytoplasmic outgrowth during terminal branching of the tracheal system. *Development* **122**, 1353-1362.

Hacohen, N., Kramer, S., Sutherland, D., Hiromi, Y. and Krasnow, M. A. (1998). *sprouty* encodes a novel antagonist of FGF signaling that patterns apical branching of the *Drosophila* airways. *Cell* **92**, 253-263.

Haller, J., Cote, S., Bronner, G. and Jackle, H. (1987). Dorsal and neural expression of a tyrosine kinase-related *Drosophila* gene during embryonic development. *Genes Dev.* **1**, 862-867.

Hiraoka, Y., Agard, D. A. and Sedat, J. W. (1990). Temporal and spatial coordination of chromosome movement, spindle formation, and nuclear envelope breakdown during prometaphase in *Drosophila* melanogaster embryos. *J. Cell Biol.* **111**, 2815-2828.

Horowitz, H. and Berg, C. A. (1996). The *Drosophila pipsqueak* gene encodes a nuclear BTB-domain-containing protein required early in oogenesis. *Development* **122**, 1859-1871.

Imam, F., Sutherland, D., Huang, W. and Krasnow, M. A. (1999). *stumps*, a *Drosophila* gene required for fibroblast growth factor (FGF)-directed migrations of tracheal and mesodermal cells. *Genetics* **152**, 307-318.

Jack, J. and Myette, G. (1997). The genes *raw* and *ribbon* are required for proper shape of tubular epithelial tissues in *Drosophila*. *Genetics* **147**, 243-253.

Kiehart, D. P., Galbraith, C. G., Edwards, K. A., Rickoll, W. L. and Montague, R. A. (2000). Multiple forces contribute to cell sheet morphogenesis for dorsal closure in *Drosophila*. *J. Cell Biol.* **149**, 471-490.

Kim, S. K. (1997). Polarized signaling: basolateral receptor localization in epithelial cells by PDZ-containing proteins. *Curr. Opin. Cell Biol.* **9**, 853-859.

Klambt, C., Glazer, L. and Shilo, B. Z. (1992). *breathless*, a *Drosophila* FGF receptor homolog, is essential for migration of tracheal and specific midline glial cells. *Genes Dev.* **6**, 1668-1678.

Kopczynski, C. C., Davis, G. W. and Goodman, C. S. (1996). A neural tetraspanin, encoded by *late bloomer*, that facilitates synapse formation. *Science* **271**, 1867-1870.

Lauffenburger, D. A. and Horwitz, A. F. (1996). Cell migration: a physically integrated molecular process. *Cell* **84**, 359-369.

Lehmann, M., Siegmund, T., Lintermann, K. G. and Korge, G. (1998). The Pipsqueak protein of *Drosophila melanogaster* binds to GAGA sequences through a novel DNA-binding domain. *J. Biol. Chem.* **273**, 28504-28509.

Lindsley, D. L. and Zimm, G. G. (1992). *The Genome of* Drosophila melanogaster. San Diego: Harcourt Brace.

Manning, G. and Krasnow, M. A. (1993). Development of the *Drosophila* Tracheal System. In *The Development of* Drosophila melanogaster. Vol. I

(ed. M. Bate and A. Martinez-Arias), pp. 609-686. New York: Cold Spring Harbor Laboratory Press.

Metzger, R. J. and Krasnow, M. A. (1999). Genetic control of branching morphogenesis. *Science* **284**, 1635-1639.

Michelson, A. M., Gisselbrecht, S., Buff, E. and Skeath, J. B. (1998). Heartbroken is a specific downstream mediator of FGF receptor signalling in *Drosophila*. *Development* **125**, 4379-4389.

Nusslein-Volhard, C., Wieschaus, E. and Kluding, H. (1984). Mutations affecting the pattern of the larval cuticle in *Drosophila melanogaster*: I. Zygotic loci on the second chromosome. *Roux's Arch. Dev. Biol.* **193**, 267-282.

Patel, N. H. (1994). Imaging neuronal subsets and other cell types in whole-mount Drosophila embryos and larvae using antibody probes. In Drosophila melanogaster*: Practical Uses in Cell and Molecular Biology*. Vol. 44 (ed. L. S. B. Goldstein and E. A. Fyrberg), pp. 446-487. San Diego: Academic Press.

Perrimon, N., Noll, E., McCall, K. and Brand, A. (1991). Generating lineage-specific markers to study *Drosophila* development. *Dev. Genet.* **12**, 238-252.

Read, D., Butte, M. J., Dernburg, A. F., Frasch, M. and Kornberg, T. B. (2000). Functional studies of the BTB domain in the *Drosophila* GAGA and Mod(mdg4) proteins. *Nucleic Acids Res.* **28**, 3864-3870.

Rebay, I. and Rubin, G. M. (1995). Yan functions as a general inhibitor of differentiation and is negatively regulated by activation of the Ras1/MAPK pathway. *Cell* **81**, 857-866.

Samakovlis, C., Hacohen, N., Manning, G., Sutherland, D. C., Guillemin, K. and Krasnow, M. A. (1996). Development of the *Drosophila* tracheal system occurs by a series of morphologically distinct but genetically coupled branching events. *Development* **122**, 1395-1407.

Sutherland, D., Samakovlis, C. and Krasnow, M. A. (1996). *branchless* encodes a *Drosophila* FGF homolog that controls tracheal cell migration and the pattern of branching. *Cell* **87**, 1091-1101.

Tepass, U., Theres, C. and Knust, E. (1990). *crumbs* encodes an EGF-like protein expressed on apical membranes of *Drosophila* epithelial cells and required for organization of epithelia. *Cell* **61**, 787-799.

Torok, T., Harvie, P. D., Buratovich, M. and Bryant, P. J. (1997). The product of *proliferation disrupter* is concentrated at centromeres and required for mitotic chromosome condensation and cell proliferation in *Drosophila*. *Genes Dev.* **11**, 213-225.

Vincent, S., Wilson, R., Coelho, C., Affolter, M. and Leptin, M. (1998). The *Drosophila* protein Dof is specifically required for FGF signaling. *Mol. Cell* **2**, 515-525.

Weber, U., Siegel, V. and Mlodzik, M. (1995). *pipsqueak* encodes a novel nuclear protein required downstream of *seven-up* for the development of photoreceptors R3 and R4. *EMBO J.* **14**, 6247-6257.

Zollman, S., Godt, D., Prive, G. G., Couderc, J. L. and Laski, F. A. (1994). The BTB domain, found primarily in zinc finger proteins, defines an evolutionarily conserved family that includes several developmentally regulated genes in *Drosophila*. *Proc. Natl. Acad. Sci. USA* **91**, 10717-10721.